

Fractional Flux Periodicity in Doped Carbon Nanotubes

K. Sasaki,^{1,*} S. Murakami,² and R. Saito³

¹*Institute for Materials Research, Tohoku University, Sendai 980-8577, Japan*

²*Department of Applied Physics, University of Tokyo, Hongo, Bunkyo-ku, Tokyo 113-8656, Japan*

³*Department of Physics, Tohoku University and CREST, JST, Sendai 980-8578, Japan*

(Dated: May 23, 2019)

An anomalous magnetic flux periodicity of the ground state is predicted in two-dimensional cylindrical surface composed of square and honeycomb lattice. The ground state and persistent currents exhibit an approximate fractional period of the flux quantum. The period depends on the aspect ratio of the cylinder and on the lattice structure around the axis. We discuss possibility of this nontrivial periodicity in a heavily doped armchair carbon nanotube.

PACS numbers: 73.23.Ra, 73.63.Fg

In the Aharonov-Bohm (AB) effect, the phase of wavefunctions is modulated by a magnetic field, thereby manifesting the quantum nature of electrons. One of the direct consequences of the AB effect in solid state physics is the persistent current in a mesoscopic ring^{1,2,3,4}. The persistent current is an equilibrium current driven by a magnetic field threading the ring, and it generally shows the flux periodicity of $\Phi_0 = hc/e$. On the other hand, there exist some systems where the period becomes a general fraction of Φ_0 , revealing an interference effect between channels. At present, theoretical investigations of the fractional flux periodicity has been done only in a two-dimensional (2D) system composed of a square lattice. Cheung et al.⁵ found that a finite length cylinder with a specific aspect ratio exhibits the fractional flux periodicity in the persistent currents. The same configuration with an additional magnetic field perpendicular to the cylindrical surface was analyzed by Choi et al.⁶ They reported that a fractional flux periodicity appears in the persistent currents. Its period is mainly determined by the additional perpendicular flux, but is also dependent on the number of lattice sites along the circumference. We have shown in the previous paper that torus geometry exhibits the fractional flux periodicity depending on the twist around the torus axis and the aspect ratio⁷.

However, since these geometries have not yet been realized experimentally, it is important to examine if existing materials with cylindrical geometry can be used to detect such an interference effect. In this paper, we will show that an approximate fractional flux periodicity appears in a honeycomb lattice cylinder, which is realized in a single wall carbon nanotube (SWNT)⁸. The fractional periodicity requires a heavy doping, shifting the Fermi energy up to the energy of the transfer integral (2.9 eV). The persistent current in doped nanotubes was also theoretically examined by Szopa et al.⁹, though they do not mention the fractional periodicity.

Here we consider the interference effect in a 2D cylinder (Fig. 1) composed of a honeycomb lattice, and calculate the ground state energy and the persistent current. The persistent current ($I_{pc}(N_\Phi)$) is defined by differentiating the ground state energy ($E_0(N_\Phi)$) with respect to the magnetic flux penetrating through a hollow core of the

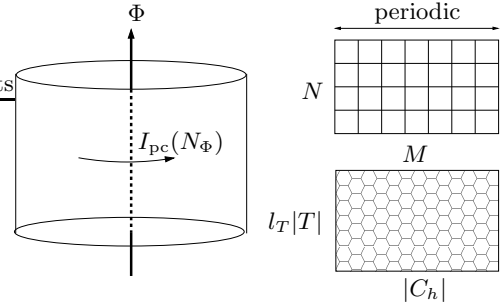


FIG. 1: (left) Geometry of a 2D cylinder in the presence of the AB flux, Φ . (right) We consider 2D cylinders composed of a square and an armchair nanotube.

cylinder (See Fig. 1) as $I_{pc}(N_\Phi) \equiv -\partial E_0(N_\Phi)/\partial \Phi$. We show that the fraction of flux period (Φ_0/Z) depends on the aspect ratio of a cylinder: $1/Z = n/l_T$ for a doped (n, n) armchair SWNT with l_T being the number of unit cells along the cylindrical axis. Persistent current can be observed experimentally via the induced magnetic moment of the system, which was recently demonstrated in a SWNT by Minot et al¹⁰.

First we consider a finite length 2D cylinder composed of a square lattice, as studied by Cheung et al⁵. The length of the cylinder and the circumferential length are Na and Ma , respectively, where a is the lattice constant. By solving the nearest-neighbor tight-binding Hamiltonian with hopping integral t , we obtain the energy eigenvalue as

$$E_{nm} = -2t \left\{ \cos \left(\frac{n\pi}{N+1} \right) + \cos \left(\frac{2\pi m}{M} \right) \right\},$$

where $1 \leq n \leq N$ and $-\frac{M}{2} + 1 \leq m \leq \frac{M}{2}$. (1)

In the presence of the AB flux parallel to the cylinder axis, E_{nm} changes according to the gauge coupling which can be obtained by substituting $m \rightarrow m - N_\Phi$ where N_Φ is the number of flux, defined by $N_\Phi \equiv \Phi/\Phi_0$ (see Fig. 1).

When we consider a half-filling system ($E_F = 0$), the

ground state energy $E_0(N_\Phi)$ is given by

$$E_0(N_\Phi) = \sum_{n=1}^N \sum_{m=[-A_n+N_\Phi]+1}^{[A_n+N_\Phi]} E_{nm}(N_\Phi), \quad (2)$$

where $A_n \equiv \frac{M}{2} \left(1 - \frac{n}{N+1}\right)$ and $[x]$ represents the largest integer smaller than x . From Eq. (2), the persistent current is expressed as

$$I_{\text{pc}}(N_\Phi) = \sum_{n=1}^N \sum_{m=[-A_n+N_\Phi]+1}^{[A_n+N_\Phi]} \frac{2et}{M} \sin\left(\frac{2\pi(m-N_\Phi)}{M}\right). \quad (3)$$

For $M \gg 1$, we can rewrite Eq. (3) as

$$\frac{I_{\text{pc}}(N_\Phi)}{I_0} = \frac{2}{M} \sum_{j=1}^{\infty} C_j \frac{\sin 2\pi N_\Phi j}{j}, \quad (4)$$

where $I_0 = 2et/(M \sin \frac{\pi}{M})$ and we ignored the correction of $\mathcal{O}(M^{-2})$ to the right hand side. The coefficient, C_j is given by

$$C_j \equiv \sum_{n=1}^N \sin\left(\frac{2\pi A_n}{M}\right) \cos(2\pi j A_n). \quad (5)$$

When the aspect ratio satisfies $M/2(N+1) = 1/Z$ with integer Z , $\cos(2\pi Z A_n) = 1$ holds for all n and C_j satisfies $C_{j+Z} = C_j$. Furthermore, in the limit of $N \gg 1$, C_Z becomes large compared with C_1, \dots, C_{Z-1} since they are proportional to $\mathcal{O}(1/N)$ and $C_Z \propto \mathcal{O}(N)$. Since only $j = Z, 2Z, \dots$ are dominant in Eq. (4), we get an approximate fractional (Φ_0/Z) periodicity of I_{pc} when $M/2(N+1) = 1/Z$ which becomes exact in the long length limit $N \gg 1$, as was found by Cheung et al.⁵

Let us apply this result to doped armchair SWNT. The carbon nanotubes can be specified by the chiral vector, $\mathbf{C}_h = n\mathbf{a}_1 + m\mathbf{a}_2$, and the translational vector, $\mathbf{T} = t_1\mathbf{a}_1 + t_2\mathbf{a}_2$, where (n, m) and (t_1, t_2) are integers and $\mathbf{a}_1, \mathbf{a}_2$ are symmetry translational vectors on the planar honeycomb lattice⁸ with $|\mathbf{a}_1|^2 = |\mathbf{a}_2|^2 = 2\mathbf{a}_1 \cdot \mathbf{a}_2$. The chiral vector \mathbf{C}_h specifies the circumference of the cylinder, and the unit cell of the nanotube is defined by two mutually perpendicular vectors \mathbf{C}_h and \mathbf{T} . The length of the cylinder is specified by a vector $l_T\mathbf{T}$. We decompose the wave vector as $\mathbf{K} = \mu_1\mathbf{K}_1 + (\mu_2/l_T)\mathbf{K}_2$ where μ_1 and μ_2 are integers, and the wave vectors \mathbf{K}_1 and \mathbf{K}_2 are defined by the periodic boundary condition: $\mathbf{C}_h \cdot \mathbf{K}_1 = 2\pi$, $\mathbf{C}_h \cdot \mathbf{K}_2 = 0$, $\mathbf{T} \cdot \mathbf{K}_1 = 0$ and $\mathbf{T} \cdot \mathbf{K}_2 = 2\pi$. With these definitions, the energy eigenvalue of the valence electrons can be expressed by

$$E_{\mu_1\mu_2}(N_\Phi) = -V_\pi \sqrt{1 + 4 \cos X \cos Y + 4 \cos^2 Y}, \quad (6)$$

where $V_\pi (= 2.9\text{eV})$ is the transfer integral for nearest-neighbor carbon atoms and the variables X and Y are

defined by

$$X = \frac{\pi}{N_c} \left(-(t_1 - t_2)(\mu_1 - N_\Phi) + (n - m) \frac{\mu_2}{l_T} \right), \quad (7)$$

$$Y = \frac{\pi}{N_c} \left(-(t_1 + t_2)(\mu_1 - N_\Phi) + (n + m) \frac{\mu_2}{l_T} \right), \quad (8)$$

where $N_c = mt_1 - nt_2$. This implies that the motions around the axis (μ_1) and along the axis (μ_2) couple with each other.

Without doping (i.e., at half-filling), the energy dispersion relation of carbon nanotube has only two distinct Fermi points called K and K' Fermi points. In this case only two channels touch the Fermi level and the ground state energy shows the AB effect with the periodicity of Φ_0 ^{11,12} and corresponding situation has reported experimentally^{10,13}. We consider a special doping which shifts the Fermi level from 0 to $E_F = \pm V_\pi$ ⁹. The energy dispersion relation around the Fermi level is approximately given by

$$E_{\mu_1\mu_2} \approx E_F - 2V_\pi \cos Y (\cos X + \cos Y). \quad (9)$$

We note that the energy dispersion relation is similar to that of the square lattice except for the factor of $\cos Y$. Here for simplicity, we adopt the armchair SWNTs ($n = m$). In the armchair SWNTs, we can set $t_1 = 1$ and $t_2 = -1$; therefore X is proportional to only μ_1 and Y to μ_2 .

We first show the numerical results of the ground state energy $E_0(N_\Phi)$ for the doped armchair SWNT. In Fig. 2(a), we plot $E_0(N_\Phi)$ of doped armchair (30, 30) SWNTs with different lengths. The ground state energy shows an approximate fractional flux periodicity depending on the aspect ratio defined by l_T/n . We can see that the approximate fractional periodicity (Φ_0/Z) corresponds to $Z = l_T/n$. However, there also exists the approximate fractional flux periodicity for a shorter nanotube, $l_T < n$ ⁷. In Fig. 2(b), we plot the ground state energy for (80, 80) armchair SWNT with $l_T = 48$ ($l_T|T| \approx 11.6[\text{nm}]$) and $l_T = 96$ ($l_T|T| \approx 23.2[\text{nm}]$). The approximate fractional periodicity corresponds to $1/Z = 1/3$ and $1/6$, respectively, in which l_T/n is $3/5$ and $6/5$.

Now we derive the fractional flux periodicity of persistent current in doped armchair SWNTs analytically with use of the result for the square lattice. Equation (1) for the square lattice is similar to Eq. (9) for the doped SWNT. Although there remains a factor of $\cos Y$ difference, it does not affect the fractional periodicity; we can analytically show below that the fractional periodicity Φ_0/Z occurs when $l_T/n = Z$ is an integer. To see this, it is useful to consider a hypothetical energy dispersion,

$$-2V_\pi |\cos Y| (\cos X + \cos Y). \quad (10)$$

This energy eigenvalue corresponds to multiplying the factor $|\cos n\pi/(N+1)|$ to the $E_{nm}(N_\Phi)$ for the square

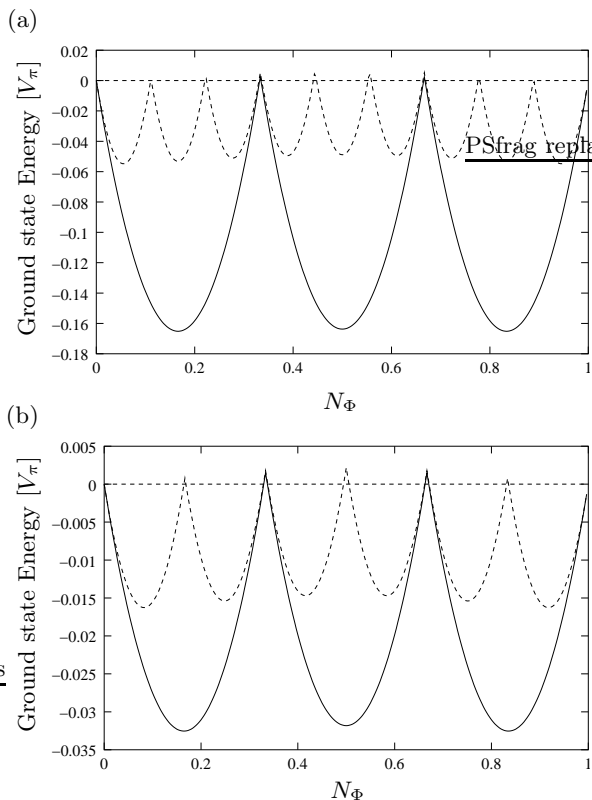


FIG. 2: Ground state energy as a function of the flux for (n, n) armchair SWNT. (a) $n = 30$ (diameter ~ 4 nm) with two different lengths: $l_T/n = 3$ (length ~ 22 nm) (solid curve), $l_T/n = 9$ (dashed curve), and (b) $n = 80$ (diameter ~ 10 nm) with two different lengths: $l_T/n = 0.6$ (length ~ 11.6 nm) (solid curve), $l_T/n = 1.2$ (dashed curve). We offset the origin of the energy for comparison.

lattice. The corresponding persistent current can be expressed by multiplying C_j in Eq. (4) by the factor of $|\cos n\pi/(N+1)|$,

$$C_j = \sum_{n=1}^N \left| \cos \frac{n\pi}{N+1} \right| \sin \left(\frac{2\pi A_n}{M} \right) \cos(2\pi j A_n). \quad (11)$$

Thus the persistent current for Eq. (10) still exhibits the fractional periodicity depending on the aspect ratio. To compare Eq. (9) with Eq. (10), we consider the difference between the ground state energies for the two energy dispersions. Figure 3 shows the occupied states (gray color) for (a) the hypothetical energy dispersion of Eq. (10) and (b) that for doped SWNT. From this figure, it follows that the difference of ground state energies is a constant independent of N_Φ , because it corresponds to the sum of energy of all states for dispersion Eq. (10) within the region of $-\pi \leq X \leq \pi$ and $\pi/2 \leq Y \leq \pi$. This shows that the persistent current in the doped armchair SWNTs has the same periodicity as the square-lattice cylinder after the replacement $t \rightarrow V_\pi$, $M \rightarrow 2n$ and $N+1 \rightarrow l_T$; the period is thus given by Φ_0/Z for an integer value of

$$Z = l_T/n.$$

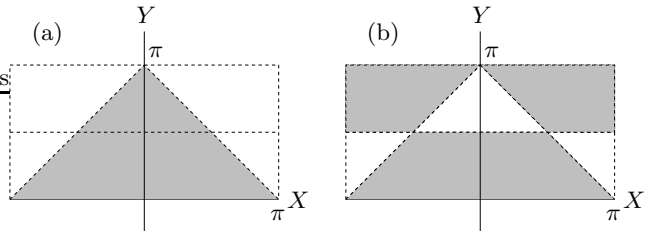


FIG. 3: Occupied states are shown in gray color in the Brillouin zone for the energy dispersion relations; (a) $-2V_\pi |\cos Y|(\cos X + \cos Y)$ in Eq. (10) and (b) $-2V_\pi \cos Y(\cos X + \cos Y)$ in Eq. (9).

Let us comment on the magnetic field B_n for (n, n) armchair SWNT which corresponds to $\Phi_0 = 4 \times 10^{-7} [\text{gauss} \cdot \text{cm}^2]$. For $n = 100$ (diameter is about 13 nm), B_n is about 30T, which is experimentally attainable. For the fractional periodicity, the period becomes $B_n/Z \sim 30\text{T}/Z$, which is easily achieved in experiments for larger Z . Although Z can be large in the long length limit of an armchair SWNT ($l_T \gg n$), the periodic motion of the electron along the axis of long nanotubes may be affected by decoherence effect such as lattice deformations or defects. It is also valuable to comment on the magnetic moment (μ_{orbit}) of the system¹⁰. The magnetic moment can be calculated directly from the persistent current as $\mu_{\text{orbit}} = S I_{\text{pc}}(N_\Phi)$, where S is the cross-sectional area of the tube ($S = |\mathbf{C}_h|^2/4\pi$). When $l_T/n = Z$ (Z is an integer), we estimate that the maximum amplitude of the magnetic moment scales as $\mu_{\text{orbit}}/\mu_B = \mathcal{O}(1)n^2$, where $\mu_B = 6 \times 10^{-2} [\text{meV}/\text{T}]$ is the Bohr magneton.

The Fermi energy ($E_F = \pm V_\pi \sim \pm 2.9\text{eV}$) for doped SWNT for the fractional flux periodicity might be difficult for chemical doping, whereas it might be possible for electrochemical doping; a recent experiment of electro-chemical gating achieves Fermi energy shift of order $\pm 1\text{eV}$ ¹⁴.

Finally we point out that the fractional nature can be seen even for the smaller Fermi energy. In Fig. 4 we plot $E_0(N_\Phi)$ with a weak doping ($E_F = -V_\pi/10$) for for (60, 30) (solid curve) and (70, 30) (dashed curve) chiral nanotube with $l_T = 15$ and $l_T = 5$, respectively. These curves clearly show some coherence effects. Thus a reproducible coherence pattern of the magnetic moment may be obtained as a function of magnetic field for doped SWNTs.

It is not easy to obtain of a SWNT with the diameter of 4nm. Thus we generally need a multi-wall carbon nanotube in which the current flows only few outermost layers. In this case we need to consider an effect of a finite thickness of layers. If the periodicity comes from the some interlayer coupling, complex coherence effect would appear. In fact, there are several experimental reports on an approximately fractional flux periodicity in

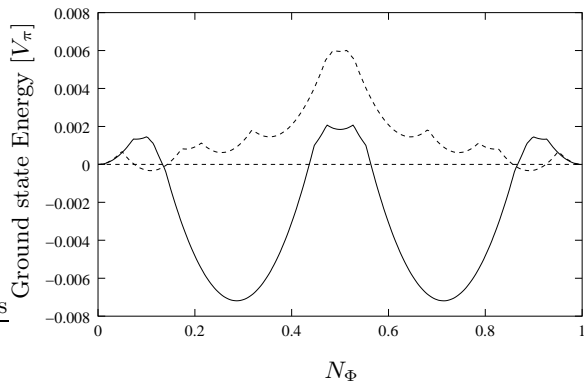


FIG. 4: Ground state energy of a weak doped ($E_F = -V_\pi/10$) chiral nanotubes. We consider (60, 30) chiral nanotube with $l_T = 15$ (solid curve) and (70, 30) with $l_T = 5$ (dashed curve). The origin of the energy has been shifted to facilitate comparison.

magneto-resistance^{15,16,17}. Bachtold et al.¹⁵ observed an oscillation with a period $\sim \Phi_0/10$. It not be explained by the Al'tshuler-Aronov-Spivak theory which predicts the period of $\Phi_0/2$ ^{15,16}. At present moment, our results do not account for these oscillations, which will be a future

work.

In conclusion, we calculated numerically and analytically the fractional periodicity of the ground state energy and persistent currents in 2D cylinders composed of a square and doped armchair SWNT. A doped armchair SWNT also exhibits the fractional periodicity when they are doped to $E_F = \pm V_\pi$. The fraction (Φ_0/Z) depends on the aspect ratio given by $Z = l_T/n$, where l_T is the number of unit cells along the cylindrical axis. An experimental investigation of the AB effect in a doped SWNT gives a key to understand this special coherence phenomenon.

Acknowledgments

K. S. is supported by a fellowship of the 21st Century COE Program of the International Center of Research and Education for Materials of Tohoku University. S. M. is supported by Grant-in-Aid (No. 16740167) from the Ministry of Education, Culture, Sports, Science and Technology, Japan. R. S. acknowledges a Grant-in-Aid (No. 13440091) from the Ministry of Education, Culture, Sports, Science and Technology, Japan.

* E-mail: sasaken@imr.tohoku.ac.jp

¹ Y. Imry, *Introduction to Mesoscopic Physics* (Oxford University Press, New York, 1997).

² M. Büttiker, Y. Imry and R. Landauer, Phys. Lett. A **96** (1983) 365; R. Landauer and M. Büttiker, Phys. Rev. Lett. **54** (1985) 2049.

³ M. Büttiker, Phys. Rev. B **32** (1985) 1846; H. F. Cheung, Y. Gefen, E. K. Riedel and W. H. Shih, Phys. Rev. B **37** (1988) 6050.

⁴ L. P. Lévy, G. Dolan, J. Dunsmuir and H. Bouchiat, Phys. Rev. Lett. **64** (1990) 2074; V. Chandrasekhar, R. A. Webb, M. J. Brady, M. B. Ketchen, W. J. Gallagher and A. Kleinsasser, Phys. Rev. Lett. **67** (1991) 3578; D. Mailly, C. Chapelier and A. Benoit, Phys. Rev. Lett. **70** (1993) 2020.

⁵ H. F. Cheung, Y. Gefen and E. K. Riedel, IBM J. Res. Develop. **32** (1988) 359.

⁶ M. Y. Choi and J. Yi, Phys. Rev. B **52** (1995) 13769.

⁷ K. Sasaki, Y. Kawazoe and R. Saito, Prog. Theor. Phys. **111** (2004) 763; cond-mat/0401597 to be published in Phys. Lett. A (2004).

⁸ R. Saito, G. Dresselhaus, and M.S. Dresselhaus, *Physical Properties of Carbon Nanotubes*, Imperial College Press, London (1998).

⁹ M. Szopa, M. Margańska and E. Zipper, Phys. Lett. A **299** (2002) 593.

¹⁰ E. D. Minot, Y. Yaish, V. Sazonova and P. L. McEuen, Nature **428** (2004) 536.

¹¹ H. Ajiki and T. Ando, J. Phys. Soc. Jpn. **62** (1993) 2470.

¹² S. Roche, G. Dresselhaus, M. S. Dresselhaus and R. Saito, Phys. Rev. B **62** (2000) 16092.

¹³ S. Zaric, G. N. Ostojic, J. Kono, J. Shaver, V. C. Moore, M. S. Strano, R. H. Hauge, R. E. Smalley and X. Wei, Science **304** (2004) 1129.

¹⁴ M. Krüger, M. R. Buiteelaar, T. Nussbaumer, C. Schönenberger, and L. Forró, Appl. Phys. Lett. **78** (2001) 1291.

¹⁵ A. Bachtold, C. Strunk, J. Salvetat, J. Bonard, L. Forro, T. Nussbaumer and C. Schönenberger, Nature, **397** (1999) 673.

¹⁶ B. L. Al'tshuler, A. G. Aronov and B. Z. Spivak, JETP Lett. **33** (1981) 94; D. Yu. Sharvin and Yu. V. Sharvin, JETP Lett. **34** (1981) 272; J. P. Carini, K. A. Muttalib and S. R. Nagel, Phys. Rev. Lett. **53** (1984) 102.

¹⁷ A. Fujiwara, K. Tomiyama, H. Suematsu, M. Yumura and K. Uchida, Phys. Rev. B **60** (1999) 13492.